Supporting Information

Signal-on Electrochemiluminescent Aptasensor Based on Target Controlled Permeable Films

Lichan Chen[a,b], Xiaoting Zeng[a], Abdul Rahim Ferhan[b], Yuwu Chi[a,*], Dong-Hwan Kim [b,*], Guonan Chen[a]

[a]MOE Key Laboratory of Analysis and Detection Technology for Food Safety, Fujian Provincial Key Laboratory of Analysis and Detection Technology for Food Safety, and Department of Chemistry, Fuzhou University, Fuzhou, Fujian, 350108, China.

[b]School of Chemical and Biomedical Engineering, Nanyang Technological University, 70 Nanyang Drive, Singapore 637457, Singapore

*E-mail: y.w.chi@fzu.edu.cn (Yuwu Chi) ; dhkim@ntu.edu.sg (Dong-Hwan Kim)

Tel: +86-591-22866137; Fax: +86-591-22866137

Experienmental section

Materials. Dicyanamide, hydrogen tetrachloroaurate trihydrate ($HAuCl_4 \cdot 3H_2O$) were purchased from Sigma. Potassium persulfate ($K_2S_2O_8$), sodium borohydride ($NaBH_4$, 96.0%) and sodium citrate were obtained from Fuchen Chemical Reagent Co. (Tianjin, China). Bisphenol A (BPA), poly(ethylenimine) (PEI, M_w~10000 and M_w~6000000), Poly(styrene sulfonic acid) sodium salt (PSS, M_w~70000), 2,2-Bis(4-hydroxyphenyl)hexafluoropropane (BPAF), Bis(4-hydroxyphenyl)sulfone (BPS), and metal salts were purchased from Aladdin Chemistry Co., Ltd. (Shanghai, China). The bisphenol A aptamer (BPA sequence: 5'-CCG GTG GGT GGT CAG GTG GGA TAG CGT TCC GCG TAT GGC CCA GCG CAT CAC GGG TTC GCA CCA-3', its secondary structure was shown in Figure S1) was obtained from Sangon Biotech Co., Ltd. (Shanghai, China). Hexestrol was purchased from TCI Tokyo Chemical Industry Co., Ltd. (Shanghai, China). All of the other chemicals were of reagent grade and used as received. 0.1 M pH 7.4 PBS containing 10 mM $K_2S_2O_8$ was used as the electrolyte in ECL analysis. Doubly distilled water was used throughout this work.

Apparatus. The preparation of bulk g-C_3N_4 was carried out in a tube furnace (GSL 1400X, Kejing Materials Technology Lt. Co., Hefei, China). TEM image of Au-g-C_3N_4 NHs was recorded on an electronic microscopy (TecnaiG2 F20S-TWIN 200 kV). The field emission scanning electron microscope (FE SEM) images of the Au-g-C_3N_4 NHs coated on glassy carbon (GC) electrodes were captured by a Nova NanoSEM 230 field-emission microscope (FEI, USA). The height of the polyelectrolyte film coated on silica substrate was characterized by atomic force microscope (AFM) (Nanoman, Veeco, Santa Barbara, CA) using tapping mode. Electrochemical (EC) and ECL measurements were carried out on an ECL detection system (MPI-E, Remex Electronic Instrument Lt. Co., Xi'an, China) with a conventional three-system composed of a GC disc working electrode (3 mm in diameter), a Pt wire counter electrode, and a Ag/AgCl (3 M KCl) reference electrode. Electrochemical impedance spectroscopy (EIS) analyses were performed with an AutoLab μAUTIII.FRA2.v electrochemical workstation (Eco Chemie, The Netherlands) in the solution of 0.1 M KNO_3 containing 20 mM $K_3[Fe(CN)_6]/K_4[Fe(CN)_6]$ using the same three-electrode system as in the ECL detection.

Synthesis of Au-g-C_3N_4 NHs. The synthesis of Au-g-C_3N_4 nanohybrids was adapted from our previous work.[1] Briefly, 10 μL of 0.01 M $HAuCl_4$ solution was added to 2 mL of the as-prepared g-C_3N_4 nanosheets suspension,[2] under stirring. The suspension was sonicated for 10 min followed by a 2 h stirring period at room temperature, and this process was repeated 3 times to ensure the formation of high dispersed AuNPs on the surface of g-C_3N_4 nanosheets. Afterward, 25 μL of 0.01 M freshly prepared $NaBH_4$ solution was added quickly to the suspension to reduce the $AuCl_4^-$, followed by continuously stirring for 20 min. Then, 10 μL of 0.01 M sodium citrate solution was added dropwise into the above suspension to improve the stability of as-prepared Au-g-C_3N_4 nanohybrids, and the stirring was maintained for 30 min. To remove excess $NaBH_4$, sodium citrate, and unbound gold nanoparticles, the obtained nanohybrid materials were centrifuged, washed thoroughly with distilled water, and finally redispersed into 1 mL of water for further use and characterization. The obtained Au-g-C_3N_4 nanohybrids possessed good dispersibility and stability in water due to the electrostatic repulsion.

Layer-by-layer assembly of polyelectrolytes on Au-g-C_3N_4 nanohybrids on GCE. Solution of PEI and PSS at 2 mg mL^{-1}, and BPA aptamer at 0.2 mg mL^{-1} were prepared in 10 mM PBS (pH 7.0). Prior to each step, the GCE was successively polished using 0.3 and 0.05 μm alumina slurry, and then washed ultrasonically in water for a few minutes. Then 3 μL of the as-prepared Au-g-C_3N_4 nanohybrids suspension was dropped onto the pretreated GCE and dried at room temperature for over 3 h. The modified electrodes were washed with 10 mM PBS (pH 7.0) to remove unabsorbed materials and immediately immersed into PEI solution for 8 min followed by two rinsing steps (5 min each) in wash beakers. This procedure was then carried out for the next polyelectrolyte. During assembly in BPA aptamer solution, the incubation time was extended to 20 min. The as-prepared electrodes were stored in 10 mM PBS (pH 7.0) in the dark prior to target binding.

Target binding. BPA solution of various concentrations was prepared in the binding buffer (25 mM Tris-HCl, pH 8.0, 100 mM NaCl, 25 mM KCl, 10 mM $MgCl_2$). The as-prepared $[(PEI/PSS)_m(PEI/Aptamer)_n]$/Au-g-$C_3N_4$ NHs/GCE was immersed in BPA solution for 40min followed by rinsed throughout with water and kept in 10 mM PBS (pH 7.0) prior to ECL experiments.

ECL detection. The ECL responses of the $[(PEI/PSS)_m(PEI/Aptamer)_n]$/Au-g-$C_3N_4$ /GCE aptasensors before and after BPA binding were recorded in 0.1 M PBS (pH 7.4) containing 10 mM $K_2S_2O_8$, scanning from 0 to −1.1 V with a scan rate of 100 mV s^{-1}.

AFM sample preparation. Silica substrate was cleaned using Piranha solution (3:1 sulfuric acid to hydrogen peroxide) followed by totally rinsing with double distilled water and drying under N_2 stream. The cleaned silica substrate were exposed to 10% (3-aminopropyl)triethoxysilane (APTES) in absolute ethanol for 15 min to render $–NH_2$ functionality to silica substrate. The substrate was then rinsed with ethanol and dried at 120°C for 15 min. Subsequently, the APTES-functionalized silica substrate was deposited with the polyelectrolyte film using the same process as mentioned above. Finally, the polyelectrolyte film deposited silica substrate was thoroughly rinsed with double distilled water and dried under N_2 stream.

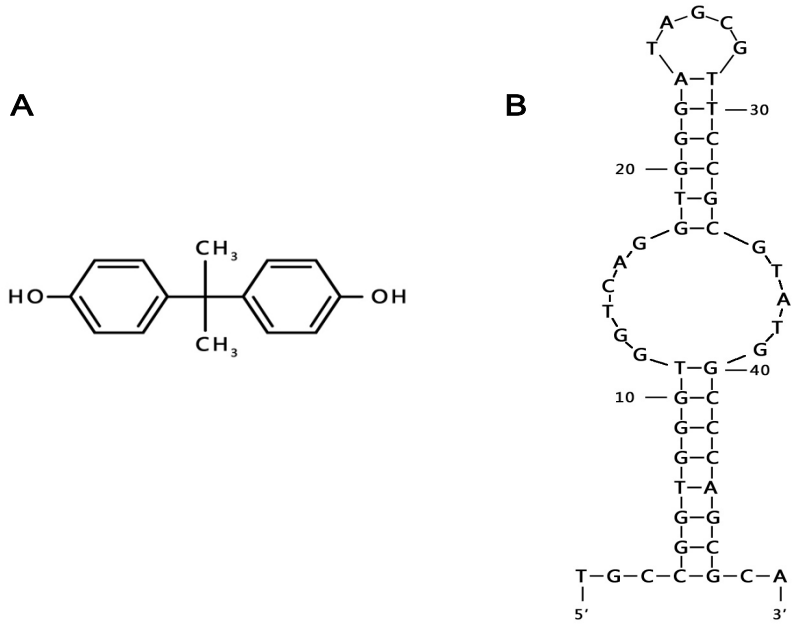

Figure S1. A) Structural formula of BPA. B) Secondary structure of the highest affinity aptamer for BPA.[3]

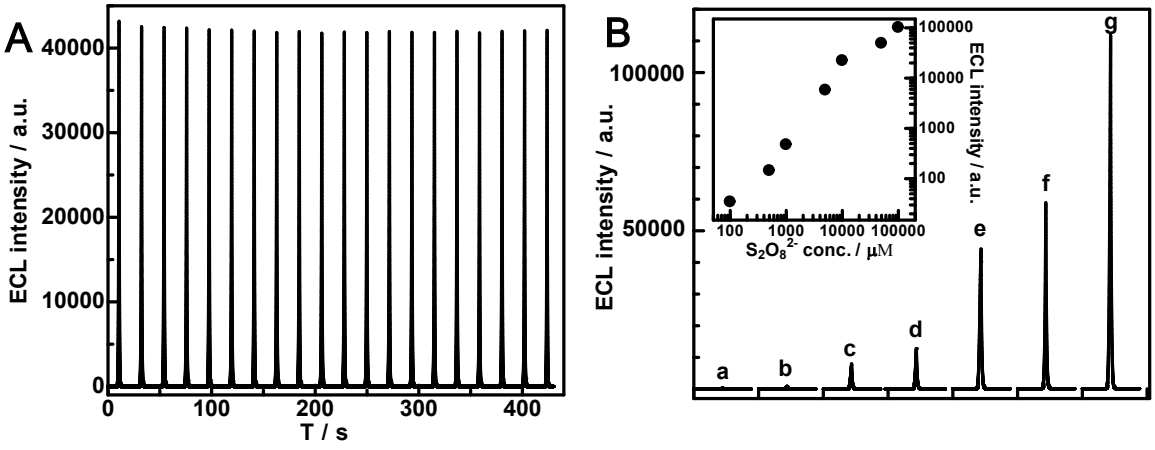

Figure S2. (A) The ECL emission of Au-g-C_3N_4 film under continuous CVs for 20 cycles with the potential range of -1.1 ~ 0 V in 100 mM PBS (pH 7.4) containing 10 mM $K_2S_2O_8$. The scan rate is 100 mV S^{-1}. (B) The $S_2O_8^{2-}$ concentration dependent Au-g-C_3N_4 ECL intensity. The ECL was tested in 100 mM PBS pH 7.4 containing a) 0.1 mM; b) 0.5 Mm; c) 1 mM; d) 5 mM; e) 10 mM; f) 50 mM; g) 100 mM $K_2S_2O_8$ with the potential range of -1.1 ~ 0 V.

Optimizing the composition of the polyelectrolyte film for constructing the sensing platform:

Using the LBL assembly technique, the thickness of the polyelectrolyte film can be precisely tuned by controlling simple variables such as polyelectrolyte selection, concentration, pH, temperature, and ionic strength.[4-6] We explored various concentrations and ionic strengths and found PEI and PSS of 2 mg mL^{-1}, and BPA aptamer of 0.2 mg mL^{-1} in 10 mM PBS (pH 7.0) to be the optimal conditions for constructing our sensing platform. As the exposure of the electroactive molecules to the electrode is dependent on the thickness of the polyelectrolyte film,[7] the layer buildup on the electrode can be readily monitored by electron-transfer resistance (R_{et}) change in electrochemical impedance spectroscopy (EIS)[8]. Figure S3A and Figure S3B showed the progression of EIS as more layers of PEI/aptamer and PEI/PSS were assembled on the Au-g-C_3N_4 film modified electrodes, respectively. R_{et} increases with the number of polyelectrolyte bilayers, indicating that multilayer polyelectrolyte film blocks the Au-g-C_3N_4 film modified electrode. Apparently, the variation of electrode passivation with the thickness of the polyelectrolyte results from that the diffusion pathways of electroactive species to the electrode surface decreases and become longer. Figure S3C summarizes the R_{et} changes *vs* number of bilayers. The smaller R_{et} change for PEI/aptamer than PEI/PSS can be attributed to different film thickness. The PSS with higher molecular weight (~ 70,000 Da) can coil in ionic solutions to form thicker layers,[6] than DNA aptamer with lower molecular weight (19,513 Da). Since the film of PEI/aptamer deposited on Au-g-C_3N_4 is thin and porous,[9] possibly making it difficult to display the effect of analyte binding on permeability, the PEI/PSS layers are required prior to the deposition of PEI/aptamer layers for assured blockage of coreactant.[9] The composition of the polyelectrolyte film was optimized to be four layers of PEI/PSS followed by six layers of PEI/aptamer (denoted as $(PEI/PSS)_4(PEI/aptamer)_6$ where the subscript refers to number of bilayers) (Figure S4). Though the ECL enhancement factor ($(I-I_0)/I_0$ (where I_0 and I refers to the ECL intensity of the $(PEI/PSS)_4(PEI/aptamer)_n$/Au-g-$C_3N_4$ film before and after target binding, respectively) of four bilayers of PEI/aptamer is a little larger than that of six bilayers (Figure S4A), six bilayers of PEI/aptamer was chosen for obtaining a wider dynamic response range, due to larger amount of aptamer embedded.

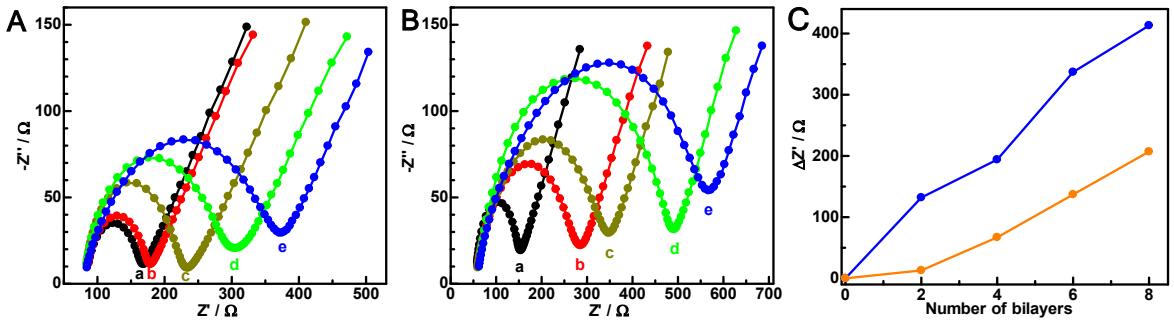

Figure S3. Monitoring layer-by-layer deposition via EIS changes. EIS of Au-g-C_3N_4 NHs-modified GC electrode with increasing rounds of PEI/aptamer (A) and PEI/PSS (B) deposition in 0.1 M KNO_3 containing 20.0 mM $K_3[Fe(CN)_6]$/ $K_4[Fe(CN)_6]$. (C) EIS change as a function of the number of bilayers of (PEI/aptamer) (orange) vs (PEI/PSS) (bule) deposition. The immersion time in EIS test solution prior to EIS measurements was 15 min.

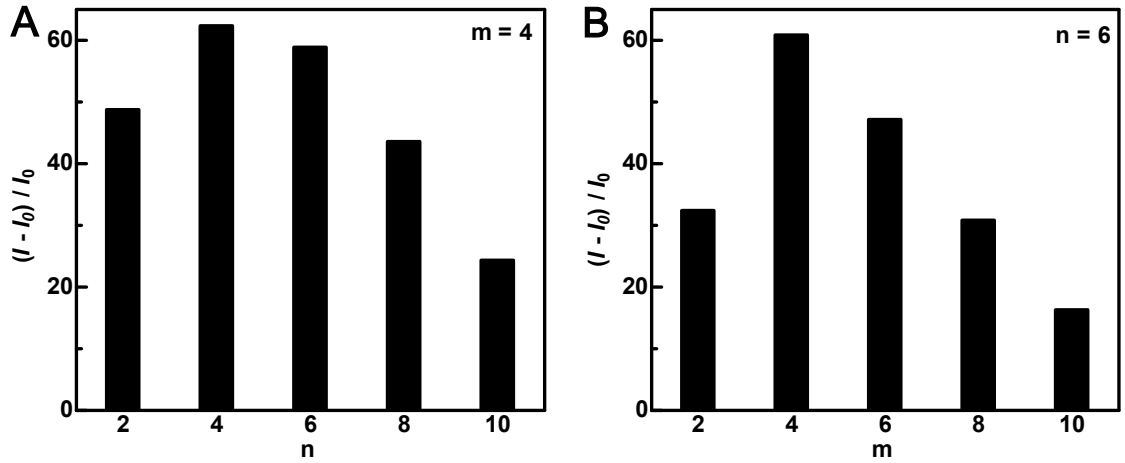

Figure S4. Optimizing the composition of the polyelectrolyte thin film $[(PEI/PSS)_m(PEI/aptamer)_n]$ via ECL enhancement factor changes upon target binding. A) Fix m = 4, change n. B) Fix n = 6, change m. The optimal film composition is $[(PEI/PSS)_4(PEI/aptamer)_6]$ for the ECL sensor. The experiments were carried out by incubating electrodes in binding buffer containing 5 ng mL^{-1} BPA for 40 min prior to ECL measurement. The immersion time in ECL test solution prior to ECL measurements was 15 min.

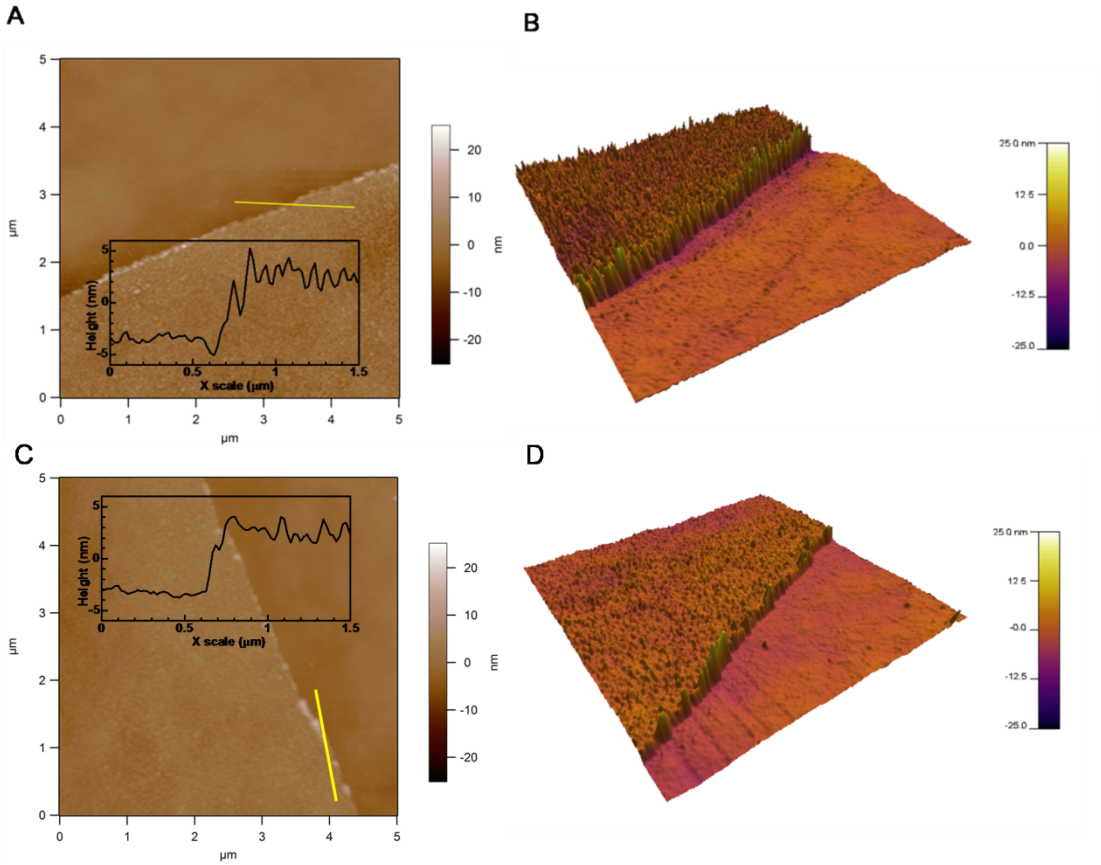

Figure S5. AFM images along the edge of an intentional scratch made in a film comprised of $(PEI/PSS)_4(PEI/aptamer)_6$ on silica substrate. (A) and (B): the $(PEI/PSS)_4(PEI/aptamer)_6$ film without BPA binding; (C) and (D): the $(PEI/PSS)_4(PEI/aptamer)_6$ film bound with 50 ng mL^{-1} BPA. (B) and (D) are 3D AFM images. The insets show the cross-section across the scratches.

Optimizing the analytical conditions including BPA binding time and sensor immersion time in ECL test solution:

Figure S6A shows the ECL intensity change of the sensor with target incubation time. While the ECL intensity of the sensor is almost unchanged in the absence of BPA, (curve (a) in Figure S6A), in the presence of BPA, the ECL intensity increases with increasing its binding time and levels off after 40 min (curve (b) in Figures S6A). 40 min was therefore selected as target incubation time in the following experiments. Mass transport through the polyelectrolyte films is purely diffusive,[10] thus it takes time to establish the equilibrium distribution of ions (e.g. $S_2O_8^{2-}$) through the films. Figure S6B shows the ECL intensity response of the BPA-bound sensor in the ECL testing solution versus time. The ECL intensity tended to be a constant value after 15 min, indicating that the diffusion of coreactant $S_2O_8^{2-}$ almost reached equilibrium. Moreover, the constant ECL intensity may suggest that the aptamer does not leak from the polyelectrolyte film, and the BPA molecules remain bound during the ECL testing process.[9, 11] As a result, 15 min was employed as immersion time in ECL test solution.

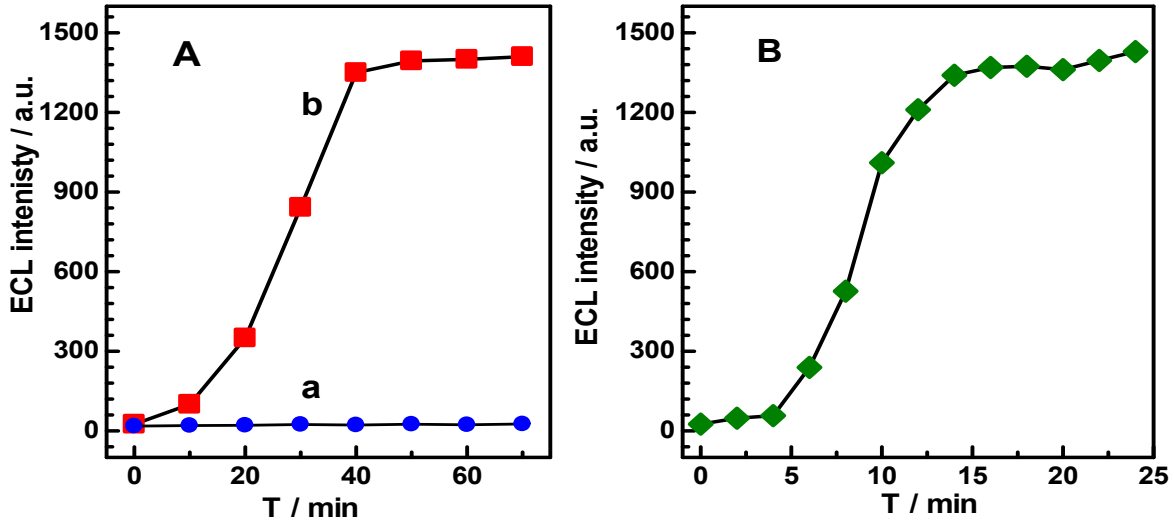

Figure S6. (A) Effect of BPA binding time on ECL responses of $[(PEI/PSS)_4(PEI/aptamer)_6]$/Au-g-$C_3N_4$ film in binding buffer without (a) and with 5 ng mL^{-1} BPA (b). The BPA bound sensors were immersed in ECL test solution for 15 min prior to ECL measurement. (B) The equilibrium time required for $S_2O_8^{2-}$ diffusion through the BPA bound polyelectrolyte film ($(PEI/PSS)_4(PEI/aptamer)_6$), which was determined by monitoring ECL response versus time. The sensor was pre-bound with 5 ng mL^{-1} BPA for 40 min before it was investigated in the ECL test solution.

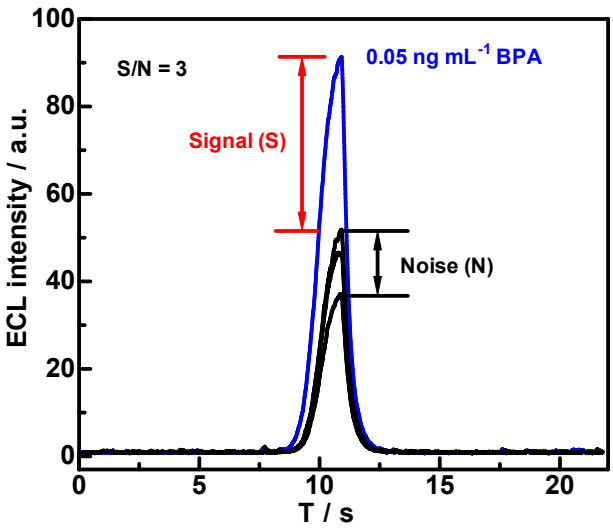

Figure S7. The limit of detection measured for the ECL aptasensor of BPA.

Table S1. Comparison of the analytical performances of the as-proposed ECL aptasensor in the detection of BPA with those of other methods.

Method	*Linear range*	*Detection limit*	*References*
This work	0.1-500 ng mL^{-1}	0.05 ng mL^{-1}	
HPLC	0.5-100 µg mL^{-1}	0.07µg mL^{-1}	12
HPLC coupled with SPE	0.2-200 ng mL^{-1}	0.083 ng mL^{-1}	13
GC	0.1-100 ng mL^{-1}	0.1 ng mL^{-1}	14
Impedimetric immunosensor	1.0-100 ng mL^{-1}	0.3 ng mL^{-1}	15
Potentiometric immunosensor	1.0-30.0 ng mL^{-1}	0.6 ng mL^{-1}	16
Electrochemical aptasensor	0.01 -10 µM	0.005 µM	17
Optofluidics based immunosensor	0.5-100 ng mL^{-1}	0.06 ng mL^{-1}	18
Evanescent wave immunosensor	0.124-9.60 ng mL^{-1}	0.03 ng mL^{-1}	19
Field effect transistor	2.19×10^{-12}–4.38×10^{-4} M		20
Surface plasmon resonance	0.05-1000 ng mL^{-1}	0.08 ng mL^{-1}	21
Chemiluminescence	0.05-50 µM	0.01µM	22
Fluorescence	0.024-0.4 µg mL^{-1}	2.0 ng mL^{-1}	23

The reusability of the sensor

Mild elution condition utilizing chelating agent was carried out for regenerating the electrode after each addition of BPA. To disruption of the BPA aptamer 3D structure, 1.0 M imidazole was applied as a complexing agent for Mg^{2+} that was added in BPA binding buffer for correct folding of the aptamer. Figure S8 shows the imidazole-induced reversible unfolding of aptamers for the elution of BPA. First, the permeability of the polyelectrolyte-aptamer film was small before binding BPA, resulting low ECL background (blue curve), then the permeability was significantly increased after binding BPA and leading to a large ECL signal (black curves). The enlarged permeability of the film due to BPA binding could be decreased again to a small value after eluting BPA with imidazole and the aptamer sensor was basically regenerated (red curves), indicating the potential for repeated use of the electrode as a practical sensor.

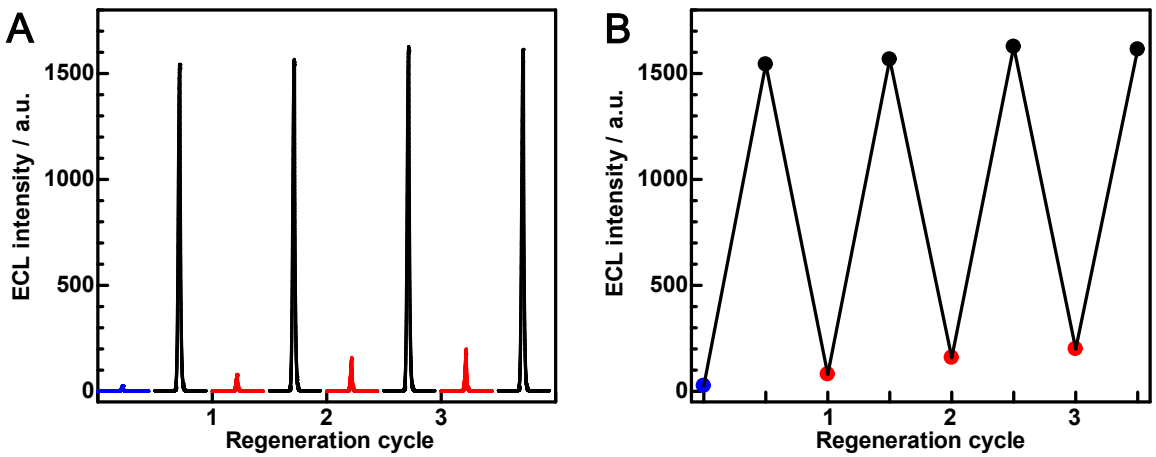

Figure S8. Regeneration of the used sensing electrode via addition of chelating agent imidazole. (A) ECL responses on the freshly prepared sensor before (blue lines) and after (black lines) sensing BPA, and on the regenerated sensor (red lines). (B) The variation of ECL intensity during BPA sensing and regeneration cycles. The Regeneration of sensor was carried out by incubating the electrode with 1.0 M imidazole in 25 mM Tris-HCl, pH 8.0, 100 mM NaCl, 0.05% Tween 20 for 20 min at room temperature. BPA concentration used for regeneration investigation was 5 ng mL^{-1}.

References

1. L. Chen, X. Zeng, P. Si, Y. Chen, Y. Chi, D.-H. Kim and G. Chen, *Anal. Chem.*, 2014, **86**, 4188-4195.
2. X. D. Zhang, X. Xie, H. Wang, J. J. Zhang, B. C. Pan and Y. Xie, *J. Am. Chem. Soc.*, 2013, **135**, 18-21.

3. M. Jo, J. Y. Ahn, J. Lee, S. Lee, S. W. Hong, J. W. Yoo, J. Kang, P. Dua, D. K. Lee, S. Hong and S. Kim, *Oligonucleotides*, 2011, **21**, 85-91.
4. Y. Lvov, K. Ariga, I. Ichinose and T. Kunitake, *J. Am. Chem. Soc.*, 1995, **117**, 6117-6123.
5. B. Schoeler, G. Kumaraswamy and F. Caruso, *Macromolecules*, 2001, **35**, 889-897.
6. A. V. Dobrynin and M. Rubinstein, *Prog. Polym. Sci.*, 2005, **30**, 1049-1118.
7. J. J. Harris and M. L. Bruening, *Langmuir*, 2000, **16**, 2006-2013.
8. A. J. Bard and L. R. Faulkner, *Electrochemical Methods: Fundamentals and Applications*, Wiley, 2000.
9. B. Malile and J. I. L. Chen, *J. Am. Chem. Soc.*, 2013, **135**, 16042-16045.
10. T. R. Farhat and J. B. Schlenoff, *J. Am. Chem. Soc.*, 2003, **125**, 4627-4636.
11. Y. Sultan and M. C. DeRosa, *Small*, 2011, **7**, 1219-1226.
12. M. Rezaee, Y. Yamini, S. Shariati, A. Esrafili and M. Shamsipur, *J. Chromatogr. A*, 2009, **1216**, 1511-1514.
13. Y. Cai, G. Jiang, J. Liu and Q. Zhou, *Anal. Chem.*, 2003, **75**, 2517-2521.
14. H.-S. Shin, C.-h. Park, S.-J. Park and H. Pyo, *J. Chromatogr. A*, 2001, **912**, 119-125.
15. M. A. Rahman, M. J. A. Shiddiky, J.-S. Park and Y.-B. Shim, *Biosens. Bioelectron.*, 2007, **22**, 2464-2470.
16. M.-H. Piao, H.-B. Noh, M. A. Rahman, M.-S. Won and Y.-B. Shim, *Electroanalysis*, 2008, **20**, 30-37.
17. L. Zhou, J. Wang, D. Li and Y. Li, *Food Chem.*, 2014, **162**, 34-40.
18. F. Long, A. Zhu, X. Zhou, H. Wang, Z. Zhao, L. Liu and H. Shi, *Biosens. Bioelectron.*, 2014, **55**, 19-25.
19. X. H. Zhou, L. H. Liu, W. Q. Xu, B. D. Song, J. W. Sheng, M. He and H. C. Shi, *Sci. Rep.*, 2014, **4**.
20. Z. C. Sánchez-Acevedo, J. Riu and F. X. Rius, *Biosens. Bioelectron.*, 2009, **24**, 2842-2846.
21. K. Hegnerova, M. Piliarik, M. Steinbachova, Z. Flegelova, H. Cernohorska and J. Homola, *Anal. Bioanal. Chem.*, 2010, **398**, 1963-1966.
22. F. Pan, L. Liu, S. Dong and C. Lu, *Spectrachim. Acta. A Mol. Biomol. Spectrosc.*, 2014, **128**, 393-397.
23. J. Fan, H. Guo, G. Liu and P. Peng, *Anal. Chim. Acta*, 2007, **585**, 134-138.